TIRSF: a web server for screening gene signatures to predict Tumor immunotherapy response

Li Chen[1,†], Tianjian Chen[1,†], Ya Zhang[1,†], Haichen Lin[1], Ruihan Wang[1], Yihang Wang[1], Hongyu Li[1], Zhixiang Zuo [2,*], Jian Ren[1,2,*] and Yubin Xie [1,*]

[1]School of Life Sciences, Institute of Precision Medicine, the First Affiliated Hospital, Sun Yat-sen University, Guangzhou 510060, China and [2]State Key Laboratory of Oncology in South China, Cancer Center, Collaborative Innovation Center for Cancer Medicine, Sun Yat-sen University, Guangzhou 510060, China

ABSTRACT

Immune checkpoint blockade (ICB) therapy has been successfully applied to clinically therapeutics in multiple cancers, but its efficacy varies greatly among different patients and cancer types. Therefore, the construction of gene signatures to identify patients who could benefit from ICB therapy is particularly important for precision cancer treatment. However, due to the lack of a user-friendly platform, the construction of such gene signatures is a great challenge for clinical investigators who have limited programming skills. In light of this challenge, we developed a web server called Tumor Immunotherapy Response Signature Finder(TIRSF) for the construction of gene signatures to predict ICB therapy response in cancer patients. TIRSF consists of three functional modules. The first module is the Signature Discovery module which provides signature construction and performance evaluation functionalities. The second is a module for response prediction based on the TIRSF signatures, which enables response prediction and prognostic analysis of immunotherapy samples. The last is a module for response prediction based on existing signatures. This module currently integrates 24 published signatures for ICB therapy response prediction. Together, all of above features can be freely accessed at **http://tirsf.renlab.org/**.

GRAPHICAL ABSTRACT
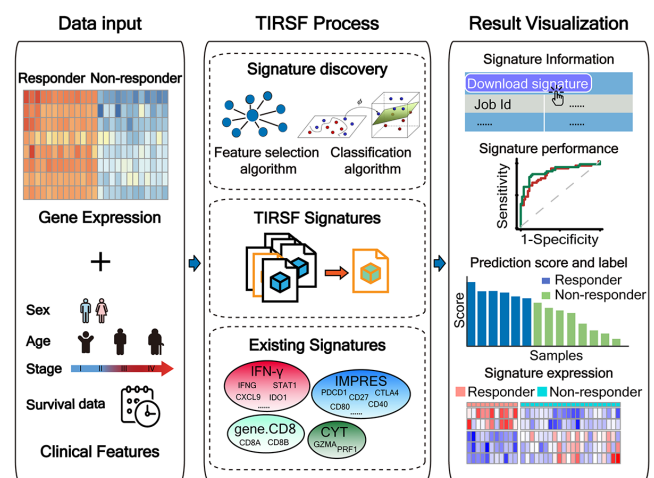
INTRODUCTION

In recent years, checkpoint blockade-based immunotherapy has offered new options and powerful weapons for cancer treatment. These therapies reactivate cytotoxic T lymphocytes (CTLs) and natural killer (NK) cells to kill cancer cells. As reported in many clinical studies, ICB therapy has achieved tremendous successes in long-term complete tumor regression in multiple malignant tumors, such as melanoma (1), non-small-cell lung carcinoma (2), and renal-cell carcinoma (3). To date, many immune checkpoints molecules, such as cytotoxic T-lymphocyte protein 4 (CTLA4) (4), programmed cell death protein 1 (PD-1) (5), PD-1 ligand (PD-L1) (6), T-cell immunoglobulin domain and mucin domain-3 (TIM-3) (7) and lymphocyte activation gene 3 (LAG-3) (8) have been studied as novel targets for intervention in clinical applications. Many immune-enhancing agents, such as ipilimumab (9), pembrolizumab (10) and atezolizumab (11), have been developed for the

blockade of these immune checkpoint molecules and have been approved for clinical treatment by FDA and NCCN guidelines. Although the concept of ICB therapy is exciting, many patients do not respond to ICB therapy (12,13) in clinical practice. Moreover, more than half of the patients experienced significant toxicity from the treatment regimen, and the survival benefit of this approach remains to be demonstrated (14,15). Therefore, the construction of an effective gene signature for a specific patient cohort that can be used to predict the outcome of ICB therapy will be particularly important in clinical practice, to provide valuable guidance for clinical individualized and precise clinical treatment.

To date, several different types of gene signatures constructed based on gene expression profiles (GEPs) have been reported in a number of published studies. Genes related to the immune suppressive microenvironment in tumors, such as fibroblast TGF-β(Pan-F-TBRS) (16) and epithelial–mesenchymal transition (EMT)-related genes (17), or genes involved in the antitumor immunity response, such as immune infiltration CD8+ T signatures (18), cytolytic activity (CYT) (19) and IFN-γ responsive genes (20), or tumor-related biomarkers such as PD-L1 expression (21) and tumor mutational burden (TMB) (22) in tumor cells, are three major types of frequently used indicators in some of the state-of-the-art gene signatures. Another category of gene expression signature was those constructed via machine learning and feature selection algorithms from differentially expressed gene sets. For example, in 2017, Pornpimol *et al.* proposed a signature selected by random forest algorithm from the genes expression profiles of 28 immune-infiltrating cells and established an immunogenicity score (IPS) to predict ICB immunotherapy response (23). Later, in 2018, Peng *et al.* (24) developed a cancer immunotherapy response prediction tool called TIDE based on the gene expression profiles of cytotoxic T lymphocytes (CTLs). Although, a number of signatures have already been developed for clinical studies, their efficacies vary greatly among different types of cancers and across individual patients. Therefore, the development of a comprehensive tool that allows users to construct response prediction signatures for ICB therapy in their own patient cohort is still a worthwhile pursuit. However, since the construction of such prediction signatures requires the use of machine learning or feature selection algorithms, it is very challenging for the clinical investigators who do not also have programming skills to perform such analyses. Moreover, to our knowledge, there are still no tools with strong interactivity and a high degree of visualization available for constructing signatures for ICB therapy prediction. In view of this, the development of an easy-to-use tool that allows users to perform not only predict ICB response but also construct response prediction signatures is still urgently needed in current clinical investigations.

In this paper, we have developed an interactive web server called TIRSF. TIRSF can automatically identify signatures to predict ICB response based on a set of feature selection and classification algorithms. An interactive heatmap was developed to visualize the signatures together with their functional annotations. If follow-up data are available, TIRSF can perform related survival analysis, and present the results using timeROC and forest plots. In addition, an-other 24 already published signatures have been integrated into TIRSF. Users can easily use this resource to predict the ICB responses of individual cancer patients.

MATERIALS AND METHODS

Data source and data preprocessing

For the evaluation of TIRSF, we collected gene expression and the corresponding clinical data from two published studies of anti-PD-1-treated melanoma patients (Supplementary Table S1) (25,26). The raw data of RNA-seq data were downloaded from the GEO (PRJEB23709) and db-GaP (phs000452) databases. The dataset with accession number of Phs000452 was used as the training set, and the PRJEB23709 dataset was used as the test set. The datasets were first downloaded from the SRA archives and then converted into fastq files with fastq-dump from SRA Toolkit v2.9.6. Quality control was performed by FastQC and low-quality reads were excluded from subsequent analysis. Reads with sufficient quality were then aligned to the hg38 human genome assembly using STAR. Expression levels were then quantified as fragments per kilobase of exon model per million mapped fragments (FPKM) for downstream analyses.

The melanoma patient response categories were defined by RECIST (Response Evaluation Criteria in Solid Tumors) as: complete response (CR) or partial response (PR) for responders, and stable disease (SD) or progressive disease (PD) for non-responders (27).

We collected 3483 immune-associated genes from canonical pathways (CP) in the Molecular Signatures Database (MSigDB) and 1019 genes from other existing signatures (Supplementary Table S2) for further analysis. After removing duplicate genes, the expression levels of 4037 genes were obtained for differential gene expression analysis (Supplementary Table S3).

Construction of the signature discovery module in TIRSF

To obtain genes that can predict the ICB therapy response status, we first selected a set of differentially expressed genes between responders and non-responders using $P < 0.05$ (limma R packages) and $|\log_2\text{fold change}| > 0.1$ as cutoffs. To construct the prediction signature, three feature selection algorithms and six classification algorithms were used. In details, a genetic algorithm, a particle swarm algorithm and recursive feature elimination were applied in the feature selection. In addition, the K-nearest neighbor (KNN), logistic regression (LR), multilayer perception (MLP), random forest (RF), support vector machine (SVM) and naïve Bayes (NB) approaches were adopted for label classification.

Construction of the response prediction module in TIRSF

Using the signature model constructed from the signature discovery module, we can obtain prediction scores and labels for input samples in the response prediction module. In this module, Kaplan–Meier analyses were performed to estimate the correlation of the of response status with overall survival (OS). The prognostic significance was estimated using the log-rank test. Time-dependent receiver operating

characteristic (ROC) analysis based on OS was performed using the 'survival' package, the 'survminer' package and the 'timeROC' (28) package in R (Version 4.0.3). Uni- and multivariate Cox regression analyses were adopted to investigate whether the prediction score was independent of other clinical features (age, sex, pathologic stage).

Constructing the module for response prediction by existing signatures

To allow users to predict ICB therapy response using other reported gene signatures, we performed an extensive literature research for studies published in recent years and collected a state-of-art set of signatures in TIRSF. Keywords including 'immune/immunotherapy', 'PD-1/PD-L1', 'biomarker/signature', 'predict/predictor', 'checkpoint' and 'response' were used in our literature search. Abstract and results sections (if necessary) were carefully scanned, and signatures that met the following two criteria were included: (i) related to immune response or resistance; and (ii) exhibits predictive potential of immunotherapy response. Finally, we collected a total of 24 transcriptomic signatures that were considered to be an ICB response indicators (Supplementary Methods, Supplementary Table S2).

RESULTS

Overview of TIRSF core functions

The TIRSF web server consists of three core functional modules. First, it contains a Signature discovery module that can find gene signatures for tumor immunotherapy response within the data provided by users. To facilitate the application of the gene signatures identified by TIRSF in clinical research, we further developed a module that we called Response Prediction by TIRSF Signatures, which enables the utilization of these signatures to predict the ICB therapy response in cancer patients. In addition to the signatures obtained from TIRSF, 24 published signatures of ICB therapy response were collected and integrated into another functional module, named Response Prediction by Existing Signatures. In this module, users can select different signatures for predicting patient ICB therapy responses and evaluate the efficacy of the signatures using prognostic data. In addition, to help researchers gain insight into the signatures of ICB therapy response, TIRSF provides a variety of analyses, including signature performance, signature expression, prognostic performance, and prognostic effect of signature. For the visualization of all analysis results, multiple statistical diagrams can be generated on the TIRSF website.

Input and output description

To identify gene signatures of ICB therapy response in the Signature discovery module, users need to input patients' transcriptome expression data of the patients and the corresponding response labels. After uploading the aforementioned input in tab-delimited format, users can create a signature discovery task by selecting different optimization and classification algorithms. The outcome will be displayed in a new interface. The displayed information includes information about the genes in the immunotherapeutic response signatures calculated by different algorithm combinations, as well as the corresponding cross-validation performances. Users can select and export the desired signature models from the results as a zip file for further analysis and use.

To predict cancer patients' ICB therapy response on the basis of the signatures identified by TIRSF, users need to upload the zip file of the signature model and gene expression profile of patients to the Response Prediction by TIRSF Signatures module. In addition, clinical features, such as survival status, follow-up time, age, and sex, can serve as additional input for further prognostic analysis of the signatures. The results page will show the signature score and the predicted immunotherapy response for each patient.

To perform response prediction on the basis of existing signatures, the gene expression profile of patients in tab-delimited format is inputted. Users can then choose signatures of interest in the interface to construct a prediction task.

All of the generated results diagrams can be exported as image files in SVG format from the TIRSF website.

Identification of tumor immunotherapy response signatures

We developed a Signature discovery module (Figure 1A) in TIRSF to identify signatures for ICB therapy responses based on gene expression profiles. To comprehensively demonstrate the function of this module, we collected data from melanoma patients treated with anti-PD-1 therapy from Liu's study (25) as examples and identified the appropriate immunotherapy response signature from this data set (Figure 1B).

We uploaded the gene expression profiles and ICB therapy response labels of these melanoma patients to the signature discovery module of TIRSF. All combinations of three optimization algorithms and six classification algorithms were used to find the optimal signature. To evaluate the performance of signatures calculated by different algorithm combinations, 4-, 6-, 8- and 10-fold cross-validations of each signature were performed in TIRSF, and the results were displayed intuitively as ROC curves and Precision-Recall (PR) curves. In the cross-validation results for the melanoma data set, the signature calculated by the recursive feature elimination algorithm and logistic regression classification algorithm, which contained 25 genes, showed the optimal performance (Figure 1B). To allow the user to choose the most appropriate result from a particular optimization algorithm and classification algorithm combination, TIRSF presents a statistical table of the basic information for each signature, including the number of genes in the signature, the name of each gene and the areas under the curve (AUCs) of the ROC curves and PR curves in the cross-validation. To provide comprehensive information on the selected signature, TIRSF will annotate each gene with the gene name and associated ID using NCBI resources. In addition, an interactive expression heatmap was developed to visualize the expression level of each gene from a selected signature in all samples.
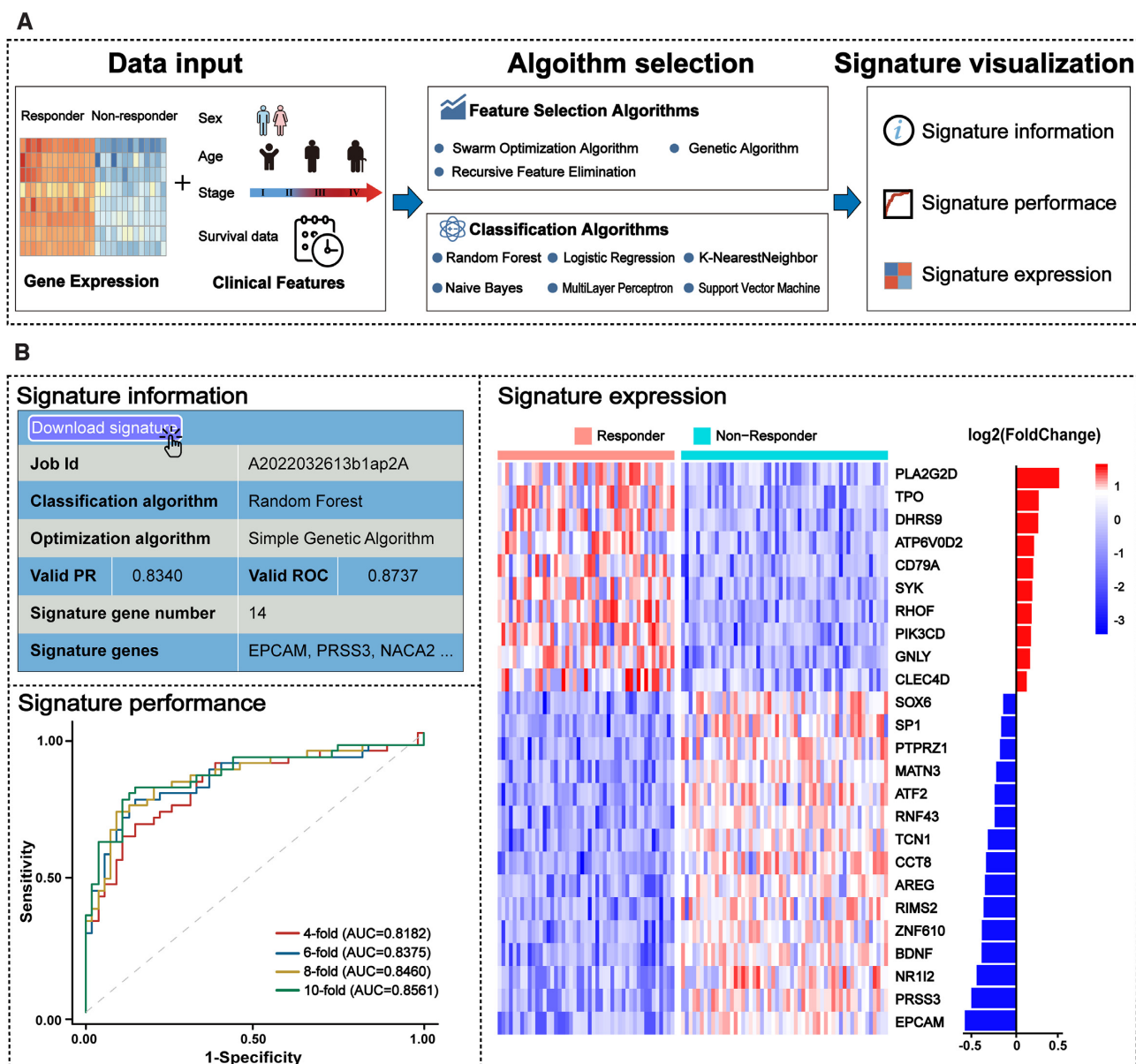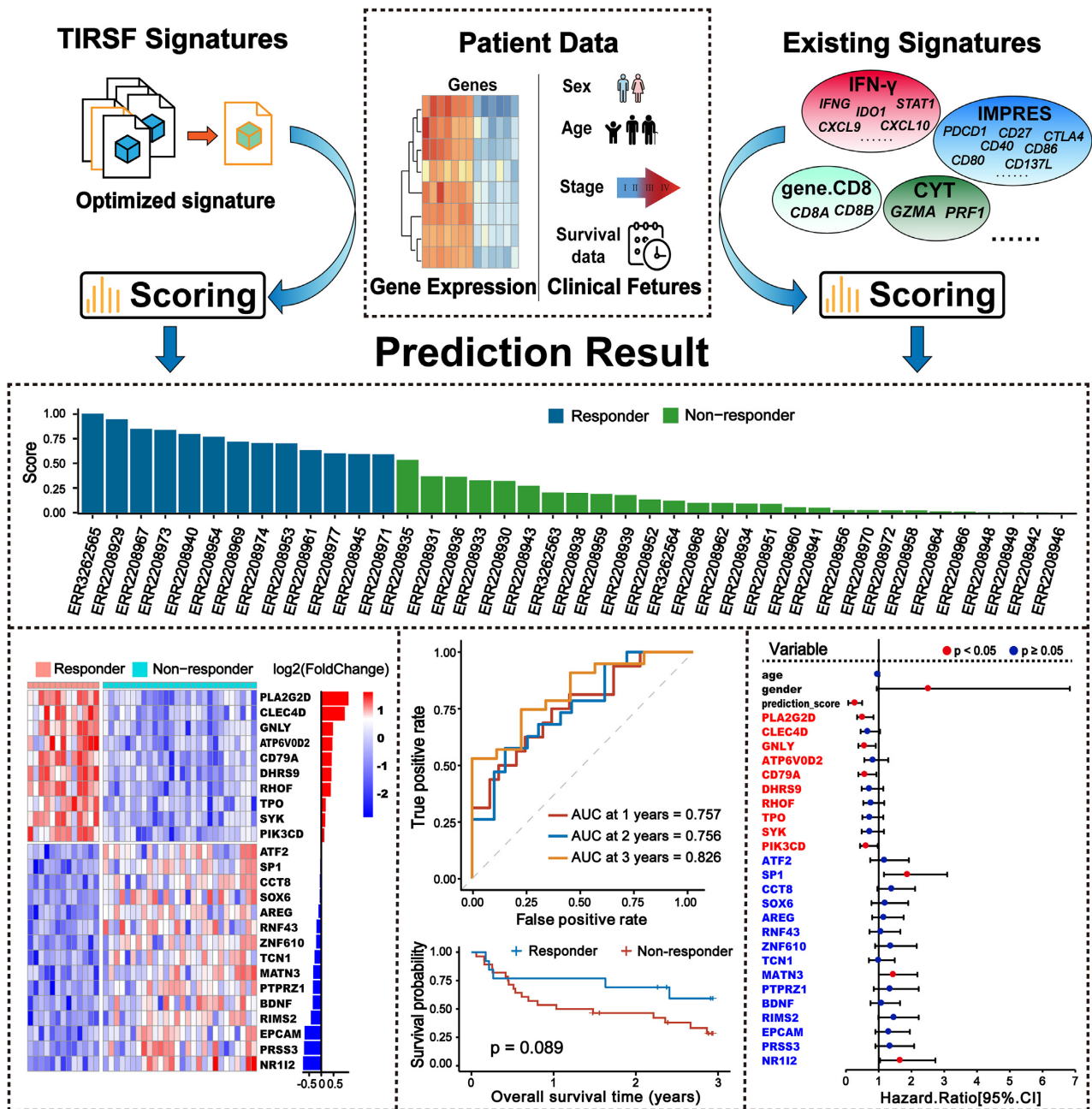
Figure 1. Signature discovery module. (**A**) Gene expression data, immunotherapy response labels, and clinical features of immunotherapy samples are needed for the Signature Discovery module in TIRSF. The signature information, signature performance, and signature expression data are displayed in the results. (**B**) Signature information, signature performance, and signature expression data for anti-PD-1 melanoma samples.

ICB therapy response prediction by TIRSF signatures

To facilitate the application of the identified signatures to ICB therapy response prediction in cancer patients, TIRSF provides the Response Prediction by TIRSF Signatures module. Figure 2 provides an example to illustrate the functionality of this module. Using the 25-gene melanoma model described above, this module calculated a signature score by logistic regression for each patient in another melanoma dataset. Then, based on the signature scores and threshold under 0.05 false positive rate in cross validation, we divided the patients into two categories, responders with scores greater than threshold and non-responders with scores below or equal to threshold, and provided a histogram in TIRSF to display the signature score of each sample. For signature model from other algorithms, TIRSF can calculated the signature score and label according to the equation and threshold defined in the model file. To reveal the differences in expression of genes in the signature between the responder and non-responder samples, TIRSF further constructed an interactive heatmap to show the gene expression level of the signature. In our example, we found that CD79A expressed significantly higher in responders. As a marker of B cell, the overexpression of CD79A implied a higher infiltration of B cells in responders. Literatures (29) were also proved that B-cell infiltration was able to sustain melanoma inflammation and may represent a better survival. Also, high level of B cell infiltrations often correlated with good response to immune checkpoint blockade

Figure 2. Response prediction by the TIRSF Signatures Discovery module and Response Prediction by Existing Signatures module. Gene expression data and clinical features of immunotherapy samples are needed for the response prediction by TIRSF signatures or existing signatures modules. Response prediction, signature expression, survival results, Cox regression results and prognostic performance of the selected signature in the melanoma test set.

therapy (30). To comprehensively evaluate the predictive effect of the signature, we also collected data on multiple clinical features of the patients and performed a series of prognostic analyses with TIRSF. First, the overall survival status and follow-up time of melanoma patients were collected as the time factors to produce the timeROC curves of the signature in TIRSF. TIRSF also presented KM curves to intuitively demonstrate the difference in prognosis between responders and non-responders. Moreover, univariate and multivariate Cox regression analyses were also performed by TIRSF to assess whether the signature or other clinical features were significantly associated with survival. In this example, Cox regression analysis of the signature was performed with two additional clinical features, age and sex, controlled. TIRSF generated forest maps containing the hazard ratio and p value of each feature to show the results of the Cox regression analysis. The Cox regression results showed that some genes in the melanoma signature were significantly correlated with the patient survival. This indicates that the signature identified by TIRSF can indeed reflect the outcomes of patients treated with ICB therapy to a certain extent.

ICB therapy response prediction by existing signatures

In addition to the response prediction by TIRSF Signatures module, 24 published signatures of ICB therapy response were implemented in another module, called Response Prediction by Existing Signatures, which allows users to directly apply these signatures to predict patients' ICB therapy response. After a user uploads the patients' expression profiles and chooses the signatures of interest, TIRSF can calculate the signature score and predict the ICB therapy response of each patient. Similarly, this module also provides a series of result visualizations, including signature prediction scores, expression heatmaps of genes in the signature, timeROC curves, KM curves, and Cox regression forest maps.

SUMMARY AND PERSPECTIVES

To help clinical investigators with limited programming skills discover gene signatures of ICB therapy response, we have developed a user-friendly tool named TIRSF, which can identify an optimal signature based on the gene expression profiles data. TIRSF is an interactive tool that not only enables the identification of ICB therapy response signatures without extensive programming knowledge but also provides a series of visual performance analyses to assist investigators in selecting the most reasonable signature. In addition, TIRSF offers a prediction module that allows the convenient prediction of patients' responses to ICB therapy according to the TIRSF signatures. We have also collected and integrated 24 additional published signatures into TIRSF so that users can apply these existing signatures to predict patient responses. To our knowledge, TIRSF is the first web server to be made available for the discovery of ICB therapy response signatures. In conclusion, TIRSF can help clinicians determine whether a patient will benefit from ICB therapy and optimize the cancer treatment strategy.

In our example data from melanoma patients, several marker genes related to tumor-infiltrating lymphocytes such as PLA2G2D and CD79A were discovered as important signature genes for immunotherapy response prediction. Recent studies (18,31,32) have revealed that tumor-infiltrating lymphocytes are important in immunotherapy and may serve as promising indicators for ICB response prediction in multiple cancers. However, in the current version of TIRSF, the construction of prediction signatures is fully data-driven. The tumor-infiltrating lymphocytes is not yet been considered in our model. Therefore, it may be a drawback needed to be solved in our next version. Given this restriction, we strongly recommended to filter the current positive predictions with actual tumor-infiltrating lymphocytes status, for example the T cell infiltration, for more reliable outcome. In the near future, we will also develop a new version of TIRSF with the tumor-infiltrating lymphocytes considered in the building of prediction signatures for ICB therapy. Computational methods for the inference of immune cell fractions, such as CIBERSORT (33), MCP-counter (34) and xcell (35), are going to integrate in this new version. By combining the tumor-infiltrating lymphocytes into the original feature, we can probably achieve a better performance for ICB therapy prediction. In addition, we will attempt to integrate other omics data, such as genomic, proteomic, and epigenomic data, into the input of TIRSF to construct more comprehensive signatures for the prediction of ICB treatment response. Also, we will optimize the calculation pipeline of TRISF to improve its calculation efficiency to better adapt to the high-dimensional characteristics of omics data. Furthermore, although there are many clinical studies on ICB therapy, there is still a lack of a comprehensive database that integrates data from these studies so that they can be fully utilized by researchers in studies of ICB therapy. Therefore, we will continue to collect cohort data and ICB therapy signatures to develop TIRSF as a comprehensive ICB therapy-related resource. We believe that with continuous improvement, TIRSF can become an effective tool for finding the precise immunotherapy response signature of diverse cancers, and can contribute to cancer treatment.

DATA AVAILABILITY

TIRSF is a web-accessible open resource available at http://tirsf.renlab.org/.

SUPPLEMENTARY DATA

Supplementary Data are available at NAR Online.

REFERENCES

1. Cuevas,L.M. and Daud,A.I. (2018) Immunotherapy for melanoma. *Semin. Cutan. Med. Surg.*, **37**, 127–131.
2. Osmani,L., Askin,F., Gabrielson,E. and Li,Q.K. (2018) Current WHO guidelines and the critical role of immunohistochemical markers in the subclassification of non-small cell lung carcinoma (NSCLC): moving from targeted therapy to immunotherapy. *Semin. Cancer Biol.*, **52**, 103–109.
3. Deleuze,A., Saout,J., Dugay,F., Peyronnet,B., Mathieu,R., Verhoest,G., Bensalah,K., Crouzet,L., Laguerre,B., Belaud-Rotureau,M.A. *et al.* (2020) Immunotherapy in renal cell carcinoma: the future is now. *Int. J. Mol. Sci.*, **21**, 2532.
4. Derakhshani,A., Hashemzadeh,S., Asadzadeh,Z., Shadbad,M.A., Rasibonab,F., Safarpour,H., Jafarlou,V., Solimando,A.G., Racanelli,V., Singh,P.K. *et al.* (2021) Cytotoxic T-Lymphocyte antigen-4 in colorectal cancer: another therapeutic side of capecitabine. *Cancers*, **13**, 2414.
5. Wang,W., Lau,R., Yu,D., Zhu,W., Korman,A. and Weber,J. (2009) PD1 blockade reverses the suppression of melanoma antigen-specific CTL by CD4+ CD25(Hi) regulatory t cells. *Int. Immunol.*, **21**, 1065–1077.

6. Yang,Y. (2015) Cancer immunotherapy: harnessing the immune system to battle cancer. *J. Clin. Invest.*, **125**, 3335–3337.

7. Sakuishi,K., Ngiow,S.F., Sullivan,J.M., Teng,M.W., Kuchroo,V.K., Smyth,M.J. and Anderson,A.C. (2013) TIM3(+)FOXP3(+) regulatory t cells are tissue-specific promoters of T-cell dysfunction in cancer. *Oncoimmunology*, **2**, e23849.

8. Wei,T., Zhang,J., Qin,Y., Wu,Y., Zhu,L., Lu,L., Tang,G. and Shen,Q. (2015) Increased expression of immunosuppressive molecules on intratumoral and circulating regulatory t cells in non-small-cell lung cancer patients. *Am. J. Cancer Res.*, **5**, 2190–2201.

9. Youssef,G. and Dietrich,J. (2020) Ipilimumab: an investigational immunotherapy for glioblastoma. *Expert Opin. Investig. Drugs*, **29**, 1187–1193.

10. Emens,L.A. (2018) Breast cancer immunotherapy: facts and hopes. *Clin. Cancer Res.*, **24**, 511–520.

11. Reddy,S.M., Carroll,E. and Nanda,R. (2020) Atezolizumab for the treatment of breast cancer. *Expert Rev. Anticancer Ther.*, **20**, 151–158.

12. Wang,Z., Goto,Y., Allevato,M.M., Wu,V.H., Saddawi-Konefka,R., Gilardi,M., Alvarado,D., Yung,B.S., O'Farrell,A., Molinolo,A.A. *et al.* (2021) Disruption of the HER3-PI3K-mTOR oncogenic signaling axis and PD-1 blockade as a multimodal precision immunotherapy in head and neck cancer. *Nat. Commun.*, **12**, 2383.

13. Koerner,J., Horvath,D., Herrmann,V.L., MacKerracher,A., Gander,B., Yagita,H., Rohayem,J. and Groettrup,M. (2021) PLGA-particle vaccine carrying TLR3/RIG-I ligand riboxxim synergizes with immune checkpoint blockade for effective anti-cancer immunotherapy. *Nat. Commun.*, **12**, 2935.

14. Larkin,J., Chiarion-Sileni,V., Gonzalez,R., Grob,J.J., Cowey,C.L., Lao,C.D., Schadendorf,D., Dummer,R., Smylie,M., Rutkowski,P. *et al.* (2015) Combined nivolumab and ipilimumab or monotherapy in untreated melanoma. *N. Engl. J. Med.*, **373**, 23–34.

15. Cetin,E.T., Tahsinoğlu,M. and Volkan,S. (1965) Epizootic of trichophyton mentagrophytes (interdigitale) in white mice. *Pathol. Microbiol. (Basel)*, **28**, 839–846.

16. Mariathasan,S., Turley,S.J., Nickles,D., Castiglioni,A., Yuen,K., Wang,Y., Kadel,E.E., Koeppen,H., Astarita,J.L., Cubas,R *et al.* (2018) TGFβ attenuates tumour response to PD-L1 blockade by contributing to exclusion of t cells. *Nature*, **554**, 544–548.

17. Leong,I. (2018) Muscle circadian clock regulates lipid storage. *Nat. Rev. Endocrinol.*, **14**, 563.

18. Tumeh,P.C., Harview,C.L., Yearley,J.H., Shintaku,I.P., Taylor,E.J., Robert,L., Chmielowski,B., Spasic,M., Henry,G., Ciobanu,V. *et al.* (2014) PD-1 blockade induces responses by inhibiting adaptive immune resistance. *Nature*, **515**, 568–571.

19. Rooney,M.S., Shukla,S.A., Wu,C.J., Getz,G. and Hacohen,N. (2015) Molecular and genetic properties of tumors associated with local immune cytolytic activity. *Cell*, **160**, 48–61.

20. Ayers,M., Lunceford,J., Nebozhyn,M., Murphy,E., Loboda,A., Kaufman,D.R., Albright,A., Cheng,J.D., Kang,S.P., Shankaran,V. *et al.* (2017) IFN-γ-related mRNA profile predicts clinical response to PD-1 blockade. *J. Clin. Invest.*, **127**, 2930–2940.

21. Herbst,R.S., Soria,J.C., Kowanetz,M., Fine,G.D., Hamid,O., Gordon,M.S., Sosman,J.A., McDermott,D.F., Powderly,J.D., Gettinger,S.N. *et al.* (2014) Predictive correlates of response to the anti-PD-L1 antibody MPDL3280A in cancer patients. *Nature*, **515**, 563–567.

22. Rizvi,N.A., Hellmann,M.D., Snyder,A., Kvistborg,P., Makarov,V., Havel,J.J., Lee,W., Yuan,J., Wong,P., Ho,T.S. *et al.* (2015) Cancer immunology. Mutational landscape determines sensitivity to PD-1 blockade in non-small cell lung cancer. *Science (New York, N.Y.)*, **348**, 124–128.

23. Charoentong,P., Finotello,F., Angelova,M., Mayer,C., Efremova,M., Rieder,D., Hackl,H. and Trajanoski,Z. (2017) Pan-cancer immunogenomic analyses reveal genotype-immunophenotype relationships and predictors of response to checkpoint blockade. *Cell Rep.*, **18**, 248–262.

24. Jiang,P., Gu,S., Pan,D., Fu,J., Sahu,A., Hu,X., Li,Z., Traugh,N., Bu,X., Li,B. *et al.* (2018) Signatures of t cell dysfunction and exclusion predict cancer immunotherapy response. *Nat. Med.*, **24**, 1550–1558.

25. Liu,D., Schilling,B., Liu,D., Sucker,A., Livingstone,E., Jerby-Arnon,L., Zimmer,L., Gutzmer,R., Satzger,I., Loquai,C. *et al.* (2019) Integrative molecular and clinical modeling of clinical outcomes to PD1 blockade in patients with metastatic melanoma. *Nat. Med.*, **25**, 1916–1927.

26. Gide,T.N., Quek,C., Menzies,A.M., Tasker,A.T., Shang,P., Holst,J., Madore,J., Lim,S.Y., Velickovic,R., Wongchenko,M. *et al.* (2019) Distinct immune cell populations define response to anti-pd-1 monotherapy and anti-pd-1/anti-ctla-4 combined therapy. *Cancer Cell*, **35**, 238–255.

27. Eisenhauer,E.A., Therasse,P., Bogaerts,J., Schwartz,L.H., Sargent,D., Ford,R., Dancey,J., Arbuck,S., Gwyther,S., Mooney,M. *et al.* (2009) New response evaluation criteria in solid tumours: revised RECIST guideline (version 1.1). *Eur. J. Cancer*, **45**, 228–247.

28. Blanche,P., Dartigues,J.F. and Jacqmin-Gadda,H. (2013) Estimating and comparing time-dependent areas under receiver operating characteristic curves for censored event times with competing risks. *Stat. Med.*, **32**, 5381–5397.

29. Griss,J., Bauer,W., Wagner,C., Simon,M., Chen,M., Grabmeier-Pfistershammer,K., Maurer-Granofszky,M., Roka,F., Penz,T., Bock,C. *et al.* (2019) B cells sustain inflammation and predict response to immune checkpoint blockade in human melanoma. *Nat. Commun.*, **10**, 4186.

30. Helmink,B.A., Reddy,S.M., Gao,J., Zhang,S., Basar,R., Thakur,R., Yizhak,K., Sade-Feldman,M., Blando,J., Han,G. *et al.* (2020) B cells and tertiary lymphoid structures promote immunotherapy response. *Nature*, **577**, 549–555.

31. Maibach,F., Sadozai,H., Seyed Jafari,S.M., Hunger,R.E. and Schenk,M. (2020) Tumor-infiltrating lymphocytes and their prognostic value in cutaneous melanoma. *Front. Immunol.*, **11**, 2105.

32. Stanton,S.E. and Disis,M.L. (2016) Clinical significance of tumor-infiltrating lymphocytes in breast cancer. *J. Immunother. Cancer*, **4**, 59.

33. Newman,A.M., Liu,C.L., Green,M.R., Gentles,A.J., Feng,W., Xu,Y., Hoang,C.D., Diehn,M. and Alizadeh,A.A. (2015) Robust enumeration of cell subsets from tissue expression profiles. *Nat. Methods*, **12**, 453–457.

34. Becht,E., Giraldo,N.A., Lacroix,L., Buttard,B., Elarouci,N., Petitprez,F., Selves,J., Laurent-Puig,P., Sautès-Fridman,C., Fridman,W.H. *et al.* (2016) Estimating the population abundance of tissue-infiltrating immune and stromal cell populations using gene expression. *Genome Biol.*, **17**, 218.

35. Aran,D., Hu,Z. and Butte,A.J. (2017) xCell: digitally portraying the tissue cellular heterogeneity landscape. *Genome Biol.*, **18**, 220.